Geophysical Research Letters

Correspondence to:
J. P. Reistad
jone.reistad@uib.no

An Explicit IMF B_y Dependence on Solar Wind-Magnetosphere Coupling

J. P. Reistad[1], K. M. Laundal[1], A. Ohma[1], T. Moretto[1], and S. E. Milan[2]

[1]Birkeland Centre for Space Science, University of Bergen, Bergen, Norway, [2]Department of Physics and Astronomy, University of Leicester, Leicester, UK

Abstract Presently, all empirical coupling functions quantifying the solar wind—magnetosphere energy—or magnetic flux conversion assume that the coupling is independent of the sign of the dawn-dusk component (B_y) of the Interplanetary Magnetic Field (IMF). In this paper we present observations strongly suggesting an explicit IMF B_y effect on the solar wind-magnetosphere coupling. When the Earth's dipole is tilted in the direction corresponding to northern winter, positive IMF B_y is found to on average lead to a larger polar cap than when IMF B_y is negative during otherwise similar conditions. This explicit IMF B_y effect is found to reverse when the Earth's dipole is inclined in the opposite direction (northern summer) and is consistently observed from both hemispheres. We interpret the different responses of the polar cap size due to the sign of IMF B_y to likely be a result of differences in the dayside reconnection rate.

1. Introduction

Today, we acknowledge opening of magnetic flux through dayside reconnection as the primary mode of energy transfer into the magnetosphere. Several attempts to quantify this energy input, or the rate of opening of magnetic flux, due to upstream Interplanetary Magnetic Field (IMF) and solar wind parameters has been made since the 1970s (Milan et al., 2012; Newell et al., 2007; Perreault & Akasofu, 1978; Tenfjord & Østgaard, 2013). Common for all such empirical coupling functions is that their dependence on the dawn-dusk component of the Interplanetary Magnetic Field (IMF B_y) is the same for both positive and negative values. This is because IMF B_y only enters the function through the magnitude of IMF (or the magnitude perpendicular to the Sun-Earth line) and through a $\sin^\alpha(\theta/2)$ term, where θ is the IMF clock angle, the angle from the Geocentric Solar Magnetic (GSM) z-axis of the IMF vector projected on the GSM yz plane, and α is a parameter depending on the specific coupling function used. Therefore, all existing empirical coupling functions exclude what we refer to as an explicit dependence on the sign of IMF B_y.

Hints of an explicit IMF B_y dependence on geomagnetic activity has been reported several times in the literature. However, the underlying physical explanation has not been firmly settled. Friis-Christensen and Wilhjelm (1975) and Vennerstrøm and Friis-Christensen (1987) were the first to notice that during northern winter, a significantly stronger westward electrojet was observed during positive IMF B_y compared to negative IMF B_y. The same effect was also noted more recently by Laundal et al. (2016) and Laundal et al. (2018a), finding the same trend in both the equivalent horizontal currents and the Birkeland currents in both hemispheres. This apparent explicit IMF B_y effect was investigated in more detail by Holappa and Mursula (2018) and Holappa et al. (2019), by investigating long time series of both the IMF and solar wind data and the AL/AU index. Although they did not conclude on an explanation for this asymmetry, they showed that it was significant and could not be explained by the Russell-McPherron effect (Russell & McPherron, 1973), which is known to seasonally modulate the occurrence of geomagnetic active times for one orientation of IMF B_y compared to the other. This effect was removed from their analysis by sorting the data based on the IMF clock angle (among other parameters) in the GSM coordinate system. They also found the explicit IMF B_y effect on ground magnetic perturbations to be more evident during local winter than summer, and more pronounced during coronal mass ejection events than the typical solar wind conditions. Holappa and Mursula (2018) quantified the explicit IMF B_y effect on the AL index in the northern hemisphere to be ~50% during the months from October–February.

The origin for this dependence of ionospheric currents on IMF B_y must be either (1) external: caused by an asymmetry in the solar wind-magnetosphere coupling affecting the dayside reconnection rate, or (2)

internal to the magnetosphere: distributing the energy and magnetic field asymmetrically (asymmetric magnetosphere-ionosphere coupling), or a combination of the two. Attempts have been made to explain the explicit IMF B_y effect solely through the latter category. Reistad et al. (2016) noted that when the dipole tilt angle and IMF B_y have the same sign, the magnetic field configuration in the closed magnetopshere becomes the most asymmetric (largest longitudinal displacement of conjugate footprints). Following Tenfjord et al. (2015), such a situation will be accompanied by an asymmetric release of magnetic stress stored in the asymmetric magnetotail, leading to stronger Birkeland currents in the crescent-shaped convection cells, consistent with the observed explicit IMF B_y effect on the westward electrojet. Friis-Christensen et al. (2017) also suggested that processes internal to the magnetosphere could explain the explicit IMF B_y effect they observed on ground magnetic perturbations. They speculated that the substorm current wedge increased more in the northern hemisphere during IMF B_y positive and in the southern hemisphere during IMF B_y negative. Finally, Laundal et al. (2018a) presented observations of the full horizontal and field-aligned current system in the ionosphere and found that the westward electrojet connected differently to the high-latitude current system during summer and winter, introducing seasonal variations in the electrojet response. They found that during summer, horizontal currents can flow across the polar cap which is illuminated. During winter, the polar cap is void of conductivity, and the horizontal currents are confined only to the auroral oval, hence enhancing the electrojet. It is therefore plausible that a significant fraction of the observed explicit IMF B_y effect on ground magnetic perturbations are related to how seasonal variations modify the magnetosphere-ionosphere coupling process.

As mentioned above, there are several mechanisms that can cause the observed explicit IMF B_y effect on ionospheric currents, all due to different aspects of the magnetosphere-ionosphere coupling. However, this does not exclude a possible contribution from an asymmetric external effect on the solar wind-magnetosphere coupling. To address that question, one must look at a quantity not severely influenced by the magnetosphere-ionosphere coupling, as is the case for magnetic perturbations associated with ionospheric currents. One such candidate is the open magnetic flux content in the magnetosphere, which at a given instance has to be equal in both polar regions to satisfy $\nabla \cdot \vec{B} = 0$.

In the Expanding/Contracting Polar Cap paradigm (e.g., Cowley & Lockwood, 1992; Milan et al., 2017) the large-scale dynamics of the magnetosphere-ionosphere system is understood as the result of opening and closure of magnetic flux on the dayside and nightside, respectively. Over sufficiently long timescales, typically a few substorm cycles, the amount of flux opened on the dayside must balance the amount of flux closed on the nightside in order to keep a finite and positive size of the polar cap. Some solar wind-magnetosphere coupling functions are designed to approximate the rate of flux opened on the dayside for given upstream conditions (e.g., Milan et al., 2012; Newell et al., 2007). While it is obvious that the long term averages of opening and closure of magnitic flux must balance, the correspondence between the average size of the open field line region (the polar cap in the ionosphere) and the long term average of the reconnection rates needs further explanation. During intervals of high dayside reconnection rates, the Earth's magnetotail needs to configure in such a way that will allow a correspondingly large nightside reconnection rate. Studies of the size of the polar cap clearly show that increasing rates of dayside opening lead to a correspondingly increasing polar cap size (Clausen et al., 2013; Green et al., 2009; Milan, 2009; Milan et al., 2015, 2009). Hence, the size of the polar cap is an indicator of the levels of dayside reconnection rate in some interval prior to the observation. While instantaneous observations show significant fluctuations from this trend, time averaged observations of the polar cap size will more accurately reflect the dayside reconnection rate during and prior to the observed interval.

In this paper we analyze the average size of the polar field-aligned current systems, assumed to reflect the variations of the polar cap size, during various levels of the average dayside reconnection rate as determined from an empirical coupling function. Our analysis enables further insight into how the sign of IMF B_y can possibly affect the rate of dayside opening of flux. Specifically we want to investigate the validity of the assumption that the sign of IMF B_y does not change the dayside reconnection rate.

2. Method
2.1. Data Selection
As we want to compute estimates of the average size of the polar cap and compare positive and negative IMF B_y situations, we need to only select observations during intervals when the dayside driving conditions are

similar for the two IMF B$_y$ polarities. This is done using a coupling function. We use the empirical coupling function derived by Milan et al. (2012) to quantify the rate of opening of flux on the dayside, Φ_D, according to the following formula:

$$\Phi_D[Wb/s] = \Lambda V_{sw}^{4/3} B_{yz} \sin^{9/2}(\theta/2), \qquad (1)$$

where $\Lambda = 3.3 \cdot 10^5$ m$^{2/3}$s$^{1/3}$, V_{sw} is the solar wind bulk velocity [km/s], B_{yz} is the magnitude of the IMF in the GSM YZ plane [nT], and θ is the IMF clock angle. To compute the value of the this coupling parameter we use solar wind and IMF observations from the OMNI database (King & Papitashvili, 2005), representing the conditions at the Earth's bow shock nose with 1 min resolution. Since the substorm cycle is an important means of transporting flux throughout the magnetosphere system, we argue that it is more relevant to consider the average dayside reconnection rate over the past few hours, $\overline{\Phi_D}$, rather than the instantaneous dayside reconnection rate, Φ_D, to reflect the instantaneous size of the polar cap. We calculate $\overline{\Phi_D}$ as the mean value in a rolling window of 2 hr before the observations at the bow shock nose. However, changing the widow size between 20 min and 4 hr does not change the conclusions from the analysis. To identify if the rolling window was dominated by a positive or negative IMF B$_y$, or neither, we require that the integrated value of Φ_D over the past 2 hr, when selecting only the 1 min observations during positive (negative) IMF B$_y$, is at least twice the integrated Φ_D when selecting the times when IMF B$_y$ was negative (positive). In this way, the rolling windows centered around times when IMF B$_y$ changes sign will be excluded, and only periods with a prevailing positive or negative IMF B$_y$ are selected. To increase the amount of IMF and solar wind data, we have linearly interpolated data gaps of up to 10 min in the OMNI data. If larger data gaps exist in the rolling window, the data point is discarded.

According to the mentioned literature, the explicit IMF B$_y$ effect is reported to occur together with a specific season. To determine the local season we use the dipole tilt angle. We define northern summer as tilt >15 and northern winter as tilt <−15, and opposite for the southern hemisphere.

2.2. Estimating the Size of the Region 1/Region 2 Current System

A best fit circle to the instantaneous maps of Birkeland currents from the Active Magnetosphere and Planetary Electrodynamics Response Experiment (AMPERE) (Anderson et al., 2000, 2008; Waters et al., 2001) is estimated for the years 2010–2016. The routine is described by Milan et al. (2015) and is an iterative approach that determines the center and radius of a circle in the polar MLAT/MLT AACGM (Altitude Adjusted Corrected GeoMagnetic) coordinate system. The iterative approach seeks to find the circle parameters minimizing the total integrated Birkeland current along the circle, hence, placing the circle between the region 1 and 2 bands of current. The inferred radius is therefore slightly larger than the radius of the polar cap. However, as demonstrated by Clausen et al. (2012), Clausen et al. (2013) and Milan et al. (2015), this boundary responds similarly as the open/closed field line boundary to opening and closure of magnetic flux. Hence, the trends seen in the variation of the fitted radius is considered to be a good proxy for the size of the polar cap.

Maps of Birkeland currents from both hemispheres are provided every 2 min from a fitting algorithm that uses a moving window of 10 min to collect the magnetic data from the Iridium satellite constellation. As the method for obtaining the circle fit of the polar cap size relies on detecting the large-scale Birkeland current system, the fit is more reliable when the large-scale Birkeland current density is not very low. We adopt the same threshold criteria as used by Milan et al. (2015), namely, that the peak-to-peak current density of the inferred integrated region 1 and 2 current bands is greater than 0.15 μA/m to be considered a reliable fit. For further details of the region 1/2 radius determination the reader is referred to Milan et al. (2015). The AMPERE radii dataset can be accessed in a public repository, see acknowledgements for details.

2.3. Computing Averages

We select all AMPERE maps during the years 2010–2016 that fit the criteria in the above two subsections and use the following subsets: Six intervals (7 kV wide) of $\overline{\Phi_D}$ starting at 0, separate the two dipole tilt orientations (±15°), separate positive and negative IMF B$_y$ orientations, and from each hemisphere separately. This lead to 48 individual subsets in which an average radius is computed. In every subset, a single peak distribution of the fitted radius is obtained. The standard deviation of the distribution of radii, σ, is between 1.3° and 2.2° latitude for all subsets. An example distribution of the subset from northern hemisphere winter during negative IMF B$_y$ and $\overline{\Phi_D} \in [7, 14]$ kV is show in Figure 1. The mean of the radius distribution is used as our metric for the average size of the region 1/2 current system rather than the median or mode, as the output from the AMPERE radius fit is represented as integer values to reflect the uncertainty in its determination.

Northern hemisphere
$-35° < \text{tilt} < -15°$
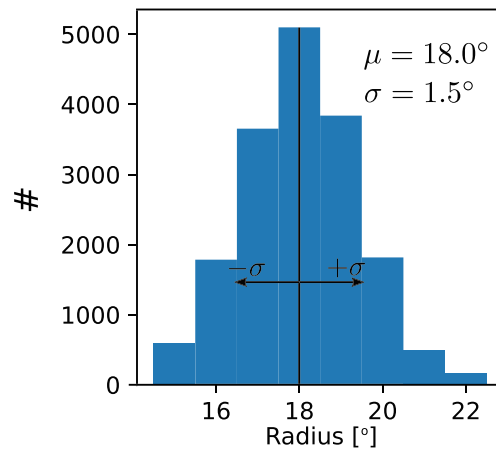IMF B_y negative
$\overline{\Phi_D} \in [14, 21]$ kV

Figure 1. Distriburion of region 1/2 radius estimates obtained from the AMPERE dataset during the years 2010–2016 from one of the subsets analyzed. The AMPERE radius is represented as integer values in the dataset to reflect the uncertainty in its determination.

3. Results

In Figure 2 we show the results obtained by averaging the radius of the region 1/2 current system from the AMPERE observations within 7 kV wide intervals of the average dayside reconnection rate $\overline{\Phi_D}$ and distinguishing periods of positive (orange) and negative (blue) dominated IMF B_y periods, as described in the previous section. The analysis for the northern hemisphere is shown in the top row of Figure 2 and the southern hemisphere analysis in the bottom row. We have performed the analysis for two intervals of the dipole tilt angle, corresponding to northern winter (left column) and northern summer (right column). In all four panels, the general trend of increasing radii for increasing $\overline{\Phi_D}$ is seen. As pointed out in the introduction, this was expected and suggests that the size of the polar cap reflects the average dayside reconnection rate in an interval prior to the observation. This close correlation between the inferred radius and $\overline{\Phi_D}$ highlights the need to examine any possible biases in $\overline{\Phi_D}$ when comparing the two IMF B_y cases (blue and orange lines in Figure 2) within the same $\overline{\Phi_D}$ interval. Due to the large number of data points, no such systematic bias exist in the presented analysis.

The sorting into intervals of $\overline{\Phi_D}$ will also take into account the Russell-McPherron effect, as $\overline{\Phi_D}$ is computed using GSM components of the IMF (Holappa & Mursula, 2018). In addition to the Russell-McPherron effect, the equinoctial effect (Cliver et al., 2000; McIntosh, 1959) is also known to lead to a semiannual modulation of geomagnetic activity. This effect is expected to maximize when the Earth's dipole axis is perpendicular to the Sun-Earth line (Cliver et al., 2000). Therefore, the dipole tilt angle, as defined in equation 15 in Laundal and Richmond (2017), is a direct measure of the proximity to this "magnetic equinox" situation. Our selection on dipole tilt angle (<-15 or >15) therefore omits the periods associated with this equinoctial maximum effect. We have also inspected the distributions of dipole tilt angle within each subset investigated. The differences of the mean dipole tilt angle between the two IMF B_y cases are all within 1° and are not systematically different for the two IMF B_y orientations.

For this paper, the most important trend seen in Figure 2 is how the two IMF B_y orientations (blue and orange lines) systematically show different radii in both hemispheres, modulated by season, namely: During negative dipole tilt (left column in Figure 2), a larger radius is observed during IMF B_y positive in both the northern and southern hemisphere. On the other hand, during positive dipole tilt (right column in Figure 2), the opposite effect is seen: A larger radius is consistently observed in both hemispheres when IMF B_y is negative compared to IMF B_y positive.

One caveat with inferring the size of the polar caps using the radius of the region 1/2 current systems is that IMF B_y alters the geometry of the current systems and could possibly give systematic differences between $\pm$ IMF B_y cases. However, as pointed out in numerous climatoligal studies (Haaland et al., 2007; Laundal, Finlay, et al., 2018a; Pettigrew et al., 2010), IMF B_y acts in the opposite sense in the two hemispheres with respect to currents and convection. Therefore, positive IMF B_y in the northern hemisphere is very similar
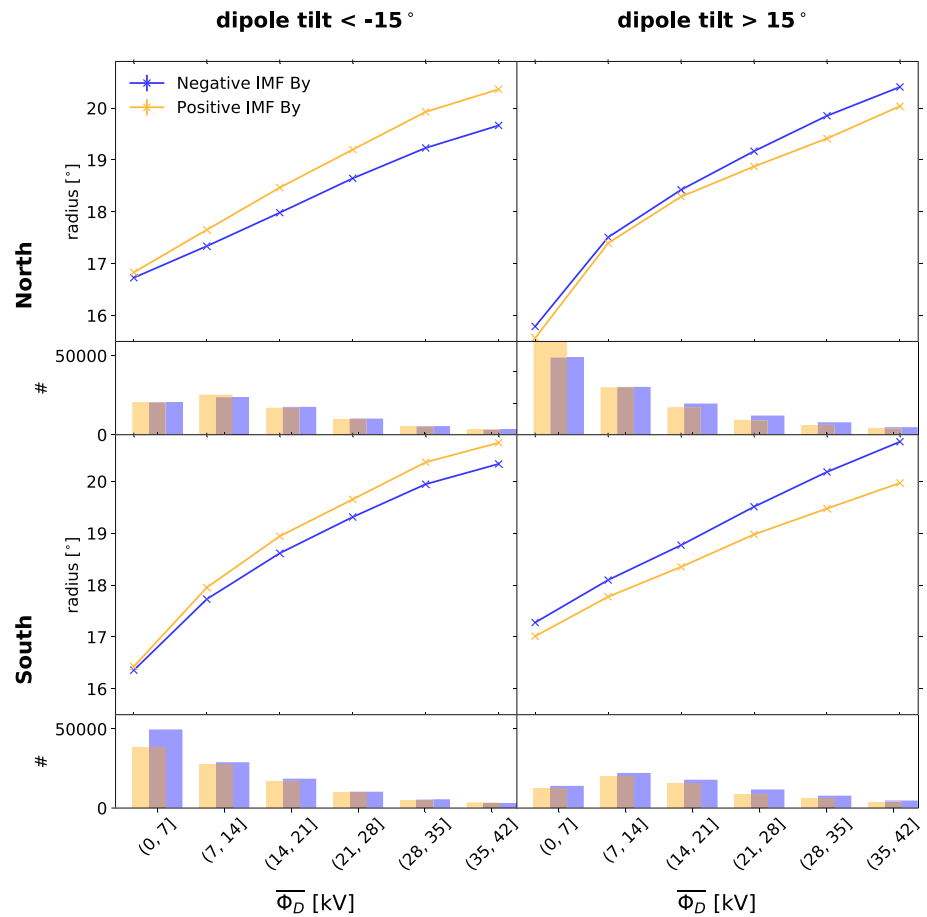
Figure 2. Radius of the region 1/2 current system as deduced from AMPERE, sorted by the average dayside reconnection rate in the 2 hr interval prior to observations, $\overline{\Phi_D}$, where periods with dominating IMF B$_y$ positive or negative interval has been separated. Top row show results from northern hemisphere while bottom row are results from southern hemisphere. Left column is during dipole tilt <−15 (northern winter and southern summer), and right column represents the opposite season in both hemispheres (dipole tilt >15). A larger radius is consistently observed in both hemispheres during IMF B$_y$ positive (negative) when dipole tilt is negative (positive). This suggests an explicit IMF B$_y$ influence on the dayside reconnection rate.

to negative IMF B$_y$ in the southern hemisphere, and vice versa, when it comes to climatology of the polar current systems. The fact that we see the same explicit IMF B$_y$ effect on the region 1/region 2 radius in the two hemispheres, rules out this interpretation of our results.

Estimating the error of the mean within each subset is challenging. This is because it is unknown when we can consider consecutive observations of the radius to be independent. We have tried to select an AMPERE circle fit only every 1 hr, reducing the dataset by a factor of 60. The overall trends are still seen. Although subsequent measurements are not entirely independent, the observations within one subset can be considered largely independent of observations within a different subset. The fact that these individual analyses (48 subsets) all show the same trend in both hemispheres during the same orientation of the dipole tilt in Figure 2 strongly indicates that the result is not due to statistical fluctuations. We present the standard error using the 2 min AMPERE resolution as vertical error bars in our Figure 2, which should be considered as a lower limit of the error of the mean. However, the standard error is smaller than the data symbol used and is hence not visible in the figure.

4. Discussion

The results shown in Figure 2 can be interpreted in two ways. The first and arguably most plausible interpretation is related to the close relationship between the size of the region 1/2 current system and the dayside reconnection rate. Since their positive correlation is firmly established, especially when consider-

ing time averaged observations (Clausen et al., 2013; Haaland et al., 2007; Milan, 2009; Milan et al., 2009, 2015; Thomas & Shepherd, 2018; Weimer, 2005), the fact that our analysis shows a clearly different size of the region 1/2 current system due to the sign of IMF B_y strongly suggests that the true dayside reconnection rate is different in the +/- IMF B_y subsets compared in Figure 2. If this is the case, empirical coupling functions designed to describe the dayside reconnection rate, such as Newell et al. (2007) and Milan et al. (2012), would benefit from including this effect depending on both the dipole tilt angle and the sign of IMF B_y.

If our interpretation of an explicit IMF B_y influence on the dayside reconnection rate is true, the previously reported explicit IMF B_y influence on ionospheric currents (Friis-Christensen & Wilhjelm, 1975; Friis-Christensen et al., 2017; Holappa & Mursula, 2018; Laundal et al., 2016; Laundal, Finlay, et al., 2018a) are likely affected by this effect. The explicit IMF B_y dependence on dayside reconnection rate suggested here would influence the ionospheric currents in the same direction as reported in the above mentioned studies. Hence, the strong explicit IMF B_y influence on ionospheric currents are not necessarily solely explained by the IMF B_y influence on the magnetosphere-ionosphere coupling during different seasons as suggested earlier but also by an explicit IMF B_y asymmetry in the solar wind-magnetosphere coupling.

A possible alternative explanation of our observations is that the magnetotail responds differently to solar wind forcing depending on the sign of IMF B_y by altering the balance between $\overline{\Phi_D}$ and open magnetic flux content. In this scenario, Φ_D does not need to depend on the sign of IMF B_y, but the combination of the sign of IMF B_y and dipole tilt modulates how much open flux the magnetosphere typically contains for the given Φ_D. While this could explain the result in Figure 2, it would not change the average nightside reconnection rate, $\overline{\Phi_N}$ since it must balance $\overline{\Phi_D}$. This means that the polar cap would be larger without any change in the circulation of plasma and magnetic flux in the ionosphere. In this case, the mentioned studies of significant explicit IMF B_y signatures on ionospheric currents would not be affected by this alternative explanation and must be solely due to aspects of the magnetosphere-ionosphere coupling. The fact that the explicit IMF B_y signatures seen on ionospheric currents in the previous mentioned studies is in the same direction as what would be expected from the first presented explanation of our results is not a definite argument against the alternative explanation. However, the dayside relation to upstream conditions are more direct compared to in the magnetotail. The more direct influence on the dayside makes the first explanation rather than the alternative one the most compelling for the authors, namely, that the combination of the sign of dipole tilt and IMF B_y can alter the dayside reconnection rate.

Both models (Hoilijoki et al., 2014; Park et al., 2006) and observations (Hoshi et al., 2018; Zhu et al., 2015) have shown that dipole tilt affects the location of the dayside reconnection line in a way that it tends to follow Earth's magnetic equatorial plane. Hoilijoki et al. (2014) showed using magnetohydrodynamic (MHD) simulations that IMF B_x can increase or reduce the tilt related displacement of the x-line, such that when tilt and IMF B_x have the same sign, the two effects can cancel and reconnection will take place close to the subsolar region, suggested to enhance the dayside reconnection rate since the magnetosheath flows are slower there (Park et al., 2006). Observations of slightly larger ionospheric currents when dipole tilt and IMF B_x have the same sign has been interpreted to be a manifestation of this effect (Laundal et al., 2018b). Due to the Parker spiral geometry of the IMF, the B_y and B_x components are anti-correlated. Hence, our results can be influenced by this B_x effect since we have not made any constraint on IMF B_x in the analysis above. To gain further insight into the source of the observed asymmetry we restricted the magnitude of the average IMF B_x in the 2 hr rolling window preceding our AMPERE observations to be less than 2 nT. This refined analysis was very little affected by this additional criterion and showed the same trend and similar magnitudes. This analysis can seen in Figure S1.

To further investigate this IMF B_x effect, we repeated the analysis by rather sorting on IMF B_x and keeping |IMF B_y| < 2 nT. The results are shown in Figure S2, on the same format as the IMF B_y analysis. In this analysis, no apparent asymmetry between the two IMF B_x orientations is seen, in contrast to Figure 2. Hence, we conclude that our results presented in Figure 2 are related to the IMF B_y component, and it is a larger effect than the IMF B_x signatures reported earlier (Laundal et al., 2018b) since we can not observe the IMF B_x effect in our analysis.

Why the sign of IMF B_y in combination with dipole tilt can have the suggested effect on dayside reconnection rate is at the moment not clear. From MHD modeling it is evident that both the dipole tilt and the IMF B_y component affect the dayside reconnection process due to the geometric north-south and dawn-dusk

asymmetries imposed on the shear angle (between draped IMF and magnetospheric field lines) and magnetosheath flow (Park et al., 2006; Trattner et al., 2012). In addition, due to the Parker spiral orientation of the IMF, the shocked solar wind has different properties pre-noon compared to post-noon, further complicating the description. Following the results from Hoilijoki et al. (2014) regarding how dipole tilt and IMF B_y change the dayside reconnection x-line location in MHD simulations, the combination of dipole tilt and IMF B_y leads to a tilted x-line that is closer to the subsolar region pre-noon and further away from the subsolar region post-noon, when dipole tilt is negative and IMF B_y positive. According to Park et al. (2006), dayside reconnection is expected to be more efficient close to the subsolar region as the magnetosheath flows are weaker here. When dipole tilt is positive and IMF B_y is negative, the pre-noon part of the x-line is also the closest to the subsolar region. For the two remaining combinations (same sign of tilt and IMF B_y), the post-noon part of the x-line is closest to the subsolar region. Therefore, if there is a slight preference for dayside reconnection to occur pre-noon due to the different plasma properties pre- and post-noon, that would be a plausible explanation of the results in Figure 2.

The aberration of the solar wind velocity due to the Earth's orbit around the Sun slightly shifts the stagnation point slightly dawnward and could possibly contribute to the observed asymmetry. We have also performed the analysis when taking the y-component of the Geocentric Solar Ecliptic (GSE) solar wind velocity into account, slightly enhancing the V_x in the Φ_D expression, and also modifying the IMF clock angle and B_{YZ} as IMF is also expressed in the aberrated coordinate system. However, the influence on the results is negligible, excluding the aberration effect as an explanation. Further analysis is needed to better understand why these combinations of dipole tilt angle and IMF B_y seem to modulate the dayside reconnection rate.

5. Conclusions

We find that the combination of dipole tilt angle and IMF B_y modulates the size of the region 1/2 current system during conditions when existing empirical coupling functions predict the same dayside reconnection rate. When dipole tilt is negative, positive IMF B_y is associated with a larger radius of the polar current systems than during negative IMF B_y. This IMF B_y dependence reverses for the opposite sign of the dipole tilt angle, and the effect is consistently observed in both hemispheres.

We suggest that this finding points at sources of variability in the dayside reconnection rate not captured by existing empirical coupling functions, as they do not take into account the sign of the IMF clock angle, nor include the dipole tilt angle. The underlying cause for these effects on dayside reconnection rate is at the moment not understood and should be further investigated.

References

Anderson, B. J., Korth, H., Waters, C. L., Green, D. L., & Stauning, P. (2008). Statistical Birkeland current distributions from magnetic field observations by the Iridium constellation. *Annales Geophysicae*, *26*(3), 671–687. https://doi.org/10.5194/angeo-26-671-2008

Anderson, B. J., Takahashi, K., & Toth, B. A. (2000). Sensing global Birkeland currents with Iridium engeneering magnetometer data. *Geophysical Research Letters*, *27*, 4045–4048.

Clausen, L. B., Milan, S. E., Baker, J. B., Ruohoniemi, J. M., Glassmeier, K. H., Coxon, J. C., & Anderson, B. J. (2013). On the influence of open magnetic flux on substorm intensity: Ground- and space-based observations. *Journal of Geophysical Research: Space Physics*, *118*, 2958–2969. https://doi.org/10.1002/jgra.50308

Clausen, L. B. N., Baker, J. B. H., Ruohoniemi, J. M., Milan, S. E., & Anderson, B. J. (2012). Dynamics of the region 1 Birkeland current oval derived from the active magnetosphere and planetary electrodynamics response experiment (AMPERE). *Journal of Geophysical Research*, *117*, 1–11. https://doi.org/10.1029/2012JA017666

Cliver, E. W., Kamide, Y., & Ling, A. G. (2000). Mountains versus valleys: Semiannual variation of geomagnetic activity. *Journal of Geophysical Research*, *105*, 2413–2424. https://doi.org/10.1029/1999JA900439

Cowley, S. W. H., & Lockwood, M. (1992). Excitation and decay of solar wind-driven flows in the magnetosphere-ionophere system. *Annales Geophysicae*, *10*(1-2), 103–115.

Friis-Christensen, E., Finlay, C. C., Hesse, M., & Laundal, K. M. (2017). Magnetic field perturbations from currents in the dark polar regions during quiet geomagnetic conditions. *Space Science Reviews*, *206*(1-4), 281–297. https://doi.org/10.1007/s11214-017-0332-1

Friis-Christensen, E., & Wilhjelm, J. (1975). Polar cap currents for different directions of the Interplanetary Magnetic Field in the Y-Z plane. *Journal of Geophysical Research*, *80*(10), 1248–1260. https://doi.org/10.1029/JA080i010p01248

Green, D. L., Waters, C. L., Anderson, B. J., & Korth, H. (2009). Seasonal and Interplanetary Magnetic Field dependence of the field-aligned currents for both northern and southern hemispheres. *Annales Geophysicae*, *27*, 1701–1715.

Haaland, S. E., Paschmann, G., Förster, M., Quinn, J. M., Torbert, R. B., McIlwain, C. E., et al. (2007). High-latitude plasma convection from Cluster EDI measurements: Mand IMF-dependence. *Annales Geophysicae*, *25*, 239–253.

Hoilijoki, S., Souza, V. M., Walsh, B. M., Janhunen, P., & Palmroth, M. (2014). Magnetopause reconnection and energy conversion as influenced by the dipole tilt and the IMF B_x. *Journal of Geophysical Research: Space Physics*, *119*, 4484–4494. https://doi.org/10.1002/2013JA019693

Holappa, L., Gopalswamy, N., & Mursula, K. (2019). Explicit IMF B$_y$—Effect maximizes at subauroral latitudes (Dedicated to the Memory of Eigil Friis-Christensen). *Journal of Geophysical Research: Space Physics*, *124*, 2854–2863. https://doi.org/10.1029/2018JA026285

Holappa, L., & Mursula, K. (2018). Explicit IMF B$_y$ dependence in high-latitude geomagnetic activity. *Journal of Geophysical Research: Space Physics*, *123*, 4728–4740. https://doi.org/10.1029/2018JA025517

Hoshi, Y., Hasegawa, H., Kitamura, N., Saito, Y., & Angelopoulos, V. (2018). Seasonal and solar wind control of the reconnection line location on the Earth's dayside magnetopause. *Journal of Geophysical Research: Space Physics*, *123*, 7498–7512. https://doi.org/10.1029/2018JA025305

King, J. H., & Papitashvili, N. E. (2005). Solar wind spatial scales in and comparisons of hourly wind and ACE plasma and magnetic field data. *Journal of Geophysical Research*, *110*, A02104. https://doi.org/10.1029/2004JA010649

Laundal, K. M., Gjerloev, J., Østgaard, N., Reistad, J., Haaland, S., Snekvik, K., et al. (2016). The impact of sunlight on high-latitude equivalent currents. *Journal of Geophysical Research: Space Physics*, *121*, 2715–2726. https://doi.org/10.1002/2015JA022236

Laundal, K. M., Finlay, C. C., Olsen, N., & Reistad, J. P. (2018a). Solar wind and seasonal influence on ionospheric currents from swarm and CHAMP measurements. *Journal of Geophysical Research: Space Physics*, *123*, 4402–4429. https://doi.org/10.1029/2018JA025387

Laundal, K. M., Reistad, J. P., Finlay, C. C., Østgaard, N., Tenfjord, P., Snekvik, K., & Ohma, A. (2018b). Interplanetary Magnetic Field B$_x$ component influence on horizontal and field-aligned currents in the ionosphere. *Journal of Geophysical Research: Space Physics*, *123*, 3360–3379. https://doi.org/10.1002/2017JA024864

Laundal, K. M., & Richmond, A. D. (2017). Magnetic coordinate systems. *Space Science Reviews*, *206*(1-4), 27–59. https://doi.org/10.1007/s11214-016-0275-y

McIntosh, D. H. (1959). On the annual variation of magnetic disturbancee. *Philosophical Transactions of the Royal Society of London Series A, Mathematical and Physical Sciences*, *251*(1001), 525–552. https://doi.org/10.1098/rsta.1959.0010

Milan, S. E. (2009). Both solar wind-magnetosphere coupling and ring current intensity control of the size of the auroral oval. *Geophysical Research Letters*, *36*, 2–5. https://doi.org/10.1029/2009GL039997

Milan, S. E., Carter, J. A., Korth, H., & Anderson, B. J. (2015). Principal component analysis of Birkeland currents determined by the active magnetosphere and planetary electrodynamics response experiment. *Journal of Geophysical Research: Space Physics*, *120*, 10,415–10,424. https://doi.org/10.1002/2015JA021680

Milan, S. E., Clausen, L. B. N., Coxon, J. C., Carter, J. A., Walach, M.-T., Laundal, K., et al. (2017). Overview of solar wind–magnetosphere–ionosphere–atmosphere coupling and the generation of magnetospheric currents. *Space Science Reviews*, 1–27. https://doi.org/10.1007/s11214-017-0333-0

Milan, S. E., Gosling, J. S., & Hubert, B. (2012). Relationship between interplanetary parameters and the magnetopause reconnection rate quantified from observations of the expanding polar cap. *Journal of Geophysical Research*, *117*, A03226. https://doi.org/10.1029/2011JA017082

Milan, S. E., Hutchinson, J., Boakes, P. D., & Hubert, B. (2009). Influences on the radius of the auroral oval. *Annales Geophysicae*, *27*(7), 2913–2924. https://doi.org/10.5194/angeo-27-2913-2009

Newell, P. T., Sotirelis, T., Liou, K., Meng, C.-I., & Rich, F. J. (2007). A nearly universal solar wind-magnetosphere coupling function inferred from 10 magnetospheric state variables. *Journal of Geophysical Research*, *112*, 1–16. https://doi.org/10.1029/2006JA012015

Park, K. S., Ogino, T., & Walker, R. J. (2006). On the importance of antiparallel reconnection when the dipole tilt and IMF B$_y$ are nonzero. *Journal of Geophysical Research: Space Physics*, *111*, 1–12. https://doi.org/10.1029/2004JA010972

Perreault, P., & Akasofu, S.-I. (1978). A study of geomagnetic storms. *Geophysical Journal of the Royal Astronomical Society*, *54*(3), 547–573. https://doi.org/10.1111/j.1365-246X.1978.tb05494.x

Pettigrew, E. D., Shepherd, S. G., & Ruohoniemi, J. M. (2010). Climatological patterns of high-latitude convection in the northern and southern hemispheres: Dipole tilt dependencies and interhemispheric comparisons. *Journal of Geophysical Research*, *115*, 1–15. https://doi.org/10.1029/2009JA014956

Reistad, J. P., Østgaard, N., Tenfjord, P., Laundal, K. M., Snekvik, K., Haaland, S., et al. (2016). Dynamic effects of restoring footpoint symmetry on closed magnetic field-lines. *Journal of Geophysical Research: Space Physics*, *121*, 1–14. https://doi.org/10.1002/2015JA022058

Russell, C. T., & McPherron, R. L. (1973). Semiannual variation of geomagnetic activity. *Journal of Geophysical Research*, *78*(1), 92–108. https://doi.org/10.1029/JA078i001p00092

Tenfjord, P., & Østgaard, N. (2013). Energy transfer and flow in the solar wind-magnetosphere-ionosphere system: A new coupling function. *Journal of Geophysical Research: Space Physics*, *118*, 5659–5672. https://doi.org/10.1002/jgra.50545

Tenfjord, P., Østgaard, N., Snekvik, K., Laundal, K. M., Reistad, J. P., Haaland, S., & Milan, S. E. (2015). How the IMF B$_y$ induces a B$_y$ component in the closed magnetosphere and how it leads to asymmetric currents and convection patterns in the two hemispheres. *Journal of Geophysical Research: Space Physics*, *120*, 9368–9384. https://doi.org/10.1002/2015JA021579

Thomas, E. G., & Shepherd, S. G. (2018). Statistical patterns of ionospheric convection derived from mid-latitude, high-latitude, and polar SuperDARN HF radar observations. *Journal of Geophysical Research: Space Physics*, *123*, 3196–3216. https://doi.org/10.1002/2018JA025280

Trattner, K. J., Petrinec, S. M., Fuselier, S. A., & Phan, T. D. (2012). The location of reconnection at the magnetopause: Testing the maximum magnetic shear model with THEMIS observations. *Journal of Geophysical Research*, *117*, 1–12. https://doi.org/10.1029/2011JA016959

Vennerstrøm, S., & Friis-Christensen, E. (1987). On the role of IMF B$_y$ in generating the electric field responsible for the flow across the polar cap. *Journal of Geophysical Research*, *92*(A1), 195. https://doi.org/10.1029/ja092ia01p00195

Waters, C. L., Anderson, B. J., & Liou, K. (2001). Estimation of global field aligned currents using the Iridium^R system magnetometer data. *Geophysical Research Letters*, *28*(11), 2165–2168. https://doi.org/10.1029/2000GL012725

Weimer, D. R. (2005). Improved ionospheric electrodynamic models and application to calculating Joule heating rates. *Journal of Geophysical Research*, *110*, A05306. https://doi.org/10.1029/2004JA010884

Zhu, C. B., Zhang, H., Ge, Y. S., Pu, Z. Y., Liu, W. L., Wan, W. X., et al. (2015). Dipole tilt angle effect on magnetic reconnection locations on the magnetopause. *Journal of Geophysical Research: Space Physics*, *120*, 5344–5354. https://doi.org/10.1002/2015JA020989